Peer-reviewed version available at Int. J. Mol. Sci. 2018, 19, 1478; doi:10.3390/ijms19051478

Article

Metformin Induces Apoptosis and Alters Cellular Responses to Oxidative Stress in HT29 Colon Cancer Cells

Paola Sena[1], Stefano Mancini[2], Marta Benincasa[1], Francesco Mariani[2], Carla Palumbo[1] and Luca Roncucci[2].

[1]Department of Biomedical, Metabolic and Neurosciences, Section of Human Morphology, [2]Department of Diagnostic and Clinical Medicine, and Public Health, University of Modena and Reggio Emilia, Policlinico, Via Del Pozzo 71, I-41125 Modena, Italy; ***paola.sena@unimore.it***, ***stefano.mancini@unimore.it***, ***marta.benincasa@unimore.it***, ***francesco.mariani@unimore.it***, ***carla.palumbo@unimore.it***, ***luca.roncucci@unimore.it***

* Correspondence: *luca.roncucci@unimore.it* Tel.: +39 0594224052

Abstract: Accumulating evidence suggests that metformin, used as an antidiabetic drug, possesses anticancer properties. Metformin reduced the incidence and growth of experimental tumors in vivo. In a randomized clinical trial among nondiabetic patients, metformin treatment significantly decreased the number of aberrant crypt foci compared to the untreated group with a follow-up of 1 month. In our study, HT29 cells were treated with graded concentrations of metformin, 10 mM/25 mM/50 mM, for 24/48 hours. We performed immunofluorescence experiments by means of confocal microscopy and Western blot analysis to evaluate a panel of factors involved in apoptotic/autophagic processes and oxidative stress response. Moreover, HT29 cells treated with metformin were analyzed by flow cytometry assay to detect the cell apoptosis rate. The results demonstrate that metformin exerts growth inhibitory effects on cultured HT29 cells by increasing both apoptosis and autophagy; moreover, it affects the survival of cultured cells inhibiting the transcriptional activation of nuclear factor E2–related factor 2 (NRF-2) and nuclear factor–kappa B (NF-κB). The effects of metformin on HT29 cells were dose- and time-dependent. These results are very intriguing, since metformin is emerging as a multifaceted drug: it has a good safety profile and is associated with low cost, and it might be a promising candidate for the prevention or treatment of colorectal cancer.

Keywords: colorectal cancer cells; metformin; apoptosis; oxidative stress

1. Introduction

Colorectal cancer (CRC) is still a major neoplasm [1], and its prevalence and mortality rate have a high impact on human health [2]. A paradigm shift from surveillance for early detection of cancer or adenomas to new preventive strategies, including chemoprevention, is necessary to reduce the burden of this disease. Several large epidemiologic and clinical studies have evaluated the possible effects of more than 200 agents, including fibers, calcium, and nonsteroidal anti-inflammatory drugs, such as 5-aminosalicylic acid and selective cyclooxygenase-2 (COX-2) inhibitors, in preventing CRC development [3]. Nonsteroidal anti-inflammatory drugs, especially COX-2 inhibitors, alone or in combination, have shown the most promise for CRC risk reduction (4), but an increased risk of serious cardiovascular events associated with COX-2 inhibitor use has been reported [5,6]. Thus, novel drugs that would be both safe and effective are needed for CRC prevention. CRC is associated with lifestyle-related diseases, such as diabetes and obesity [7–10], and these conditions might represent new targets for CRC chemoprevention. Metformin (1,1-dimethylbiguanide hydrochloride)

Peer-reviewed version available at Int. J. Mol. Sci. 2018, 19, 1478; doi:10.3390/ijms19051478

is a biguanide derivative that has long been widely used to treat diabetes mellitus [11]. It decreases basal glucose output by suppressing gluconeogenesis and glycogenolysis in the liver, and by increasing glucose uptake in muscle tissue. Because metformin does not directly stimulate insulin secretion, the risk of hypoglycemia associated with its use is lower than that associated with the use of other oral antidiabetic drugs [12]. The mechanism of action of metformin involves liver kinase B1–dependent activation of AMP-activated protein kinase [13]. Patients with type 2 diabetes taking metformin might be at lower risk of cancer (including CRC) compared with those who do not take metformin [14,15]. This evidence suggests that metformin might be a candidate agent for chemoprevention of CRC in diabetic patients. In a number of preclinical studies, metformin reduced cell proliferation, induced apoptosis, caused cell cycle arrest, and reduced incidence and growth of experimental tumors in vitro and in vivo [16,17]. Some reports also indicate that metformin improved the response of human breast tumor xenografts to conventional chemotherapy, by eradicating cancer stem cells in the tumor [18,19]. HT29 is a human colorectal adenocarcinoma cell line with epithelial morphology and represents a xenograft tumor model for colorectal cancer. Nuclear factor E2–related factor 2 (NRF-2) is a transcription factor that controls the expression of a large pool of antioxidant and cytoprotective genes regulating the cellular response to oxidative and electrophilic stress. Mutations in the *NRF-2* gene, common in cancer cells, could help tumor cells to survive and might be associated with poor survival of cancer patients. Previous studies have shown that the NRF-2 signaling pathway is abnormally activated in CRC. Nuclear factor–kappa B (NF-κB) plays a major role in linking inflammation to cancer development through its ability to upregulate several inflammatory and tumor-promoting cytokines, interleukin (IL)-6, IL-1α, and tumor necrosis factor (TNF)α, as well as genes like *BCL2* and *BCLXL*. Furthermore, NF-κB plays an important role in type 2 diabetes mellitus (T2DM), as obesity activates the transcription factor NF-κB, which increases the risk for T2DM. Collectively, NF-κB could be considered as the matchmaker between inflammation, inflammatory bowel diseases, cancer, and diabetes [20]. The present study aims to assess whether metformin has the potential to suppress the growth of colorectal cancer cells and to evaluate its role in affecting the NRF-2/NF-κB pathways.

2. Results

2.1 Metformin Suppresses Proliferation of HT29 Cells in a Dose- and Time-Dependent Manner

In order to examine whether metformin affects human colorectal cancer cell proliferation, we investigated the effect of the drug on the HT29 cancer cell line. Cells were grown in 10% fetal bovine serum and treated with increasing amounts of metformin (0, 10, 25, and 50 mmol/L). Immunofluorescence analysis was performed 24 and 48 h after adding the agents, to characterize the time-dependent impacts of metformin.

The first observation was made using inverted microscopy and concerns eventual changes of some features (viability, adhesion, morphology) of treated cells compared with controls. As shown in Figure 1, the phenotype of HT29 cells treated with metformin was preserved, although cell adhesion to the culture plates implied some changes in the characteristic rounded shape of untreated HT29 cells.

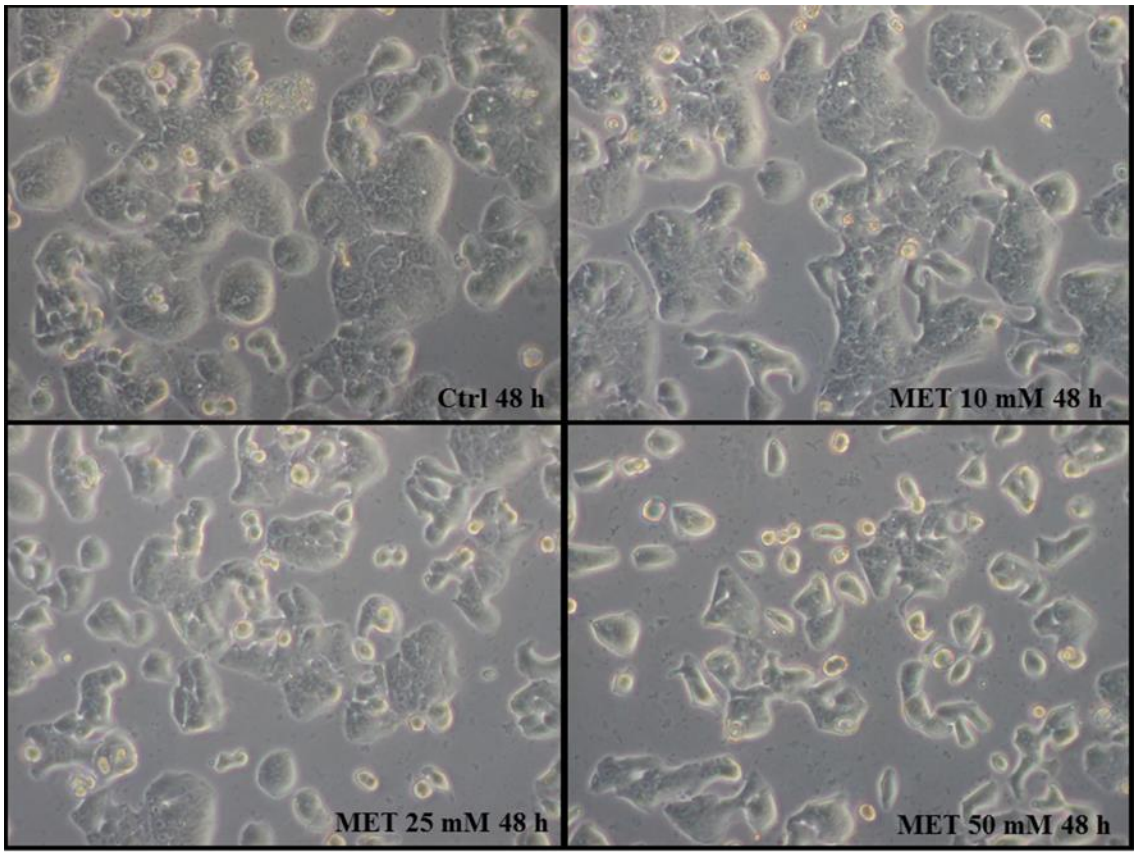

Figure 1. Inverted microscope image of HT29 cells treated with graded concentrations of metformin, 10 mM/25 mM/50 mM, for 24 h and 48 h, and of untreated cells (Ctrl). The phenotype of HT29 cells treated with metfomin was preserved, although cell adhesion to the culture plates caused some changes in the characteristic rounded shape of untreated HT29 cells.

This modification of cell morphology is probably due to the partial loss of plasma membrane attachment; these features are characteristic of the earliest phases of the apoptotic process. Cell counting showed that metformin causes a strong antiproliferative effect at a dose of 10 mM for 24 h; slight but still significant antiproliferative action was observed with higher doses for 24 h or 48 h. The following counts were obtained: 43%, 52%, and 65% inhibition for 10 mM, 25 mM, and 50 mM, respectively, after 24 h treatment compared with controls; 45%, 61%, and 68% inhibition for 10 mM, 25 mM, and 50 mM, respectively, after 48 h treatment compared with controls.

To confirm these preliminary data, immunofluorescence experiments, coupled with confocal analysis, were performed using a panel of antibodies to determine the effect of metformin treatment on the expression profile of autophagy/apoptosis or proliferation markers.

Ki-67 protein was used as ~~a~~ marker for cell proliferation, and the results from the immunofluorescence analysis (Figure 2) show that metformin significantly downregulates the expression of Ki-67 and nuclear localization in a time- and dose-dependent manner.

Peer-reviewed version available at Int. J. Mol. Sci. 2018, 19, 1478; doi:10.3390/ijms19051478

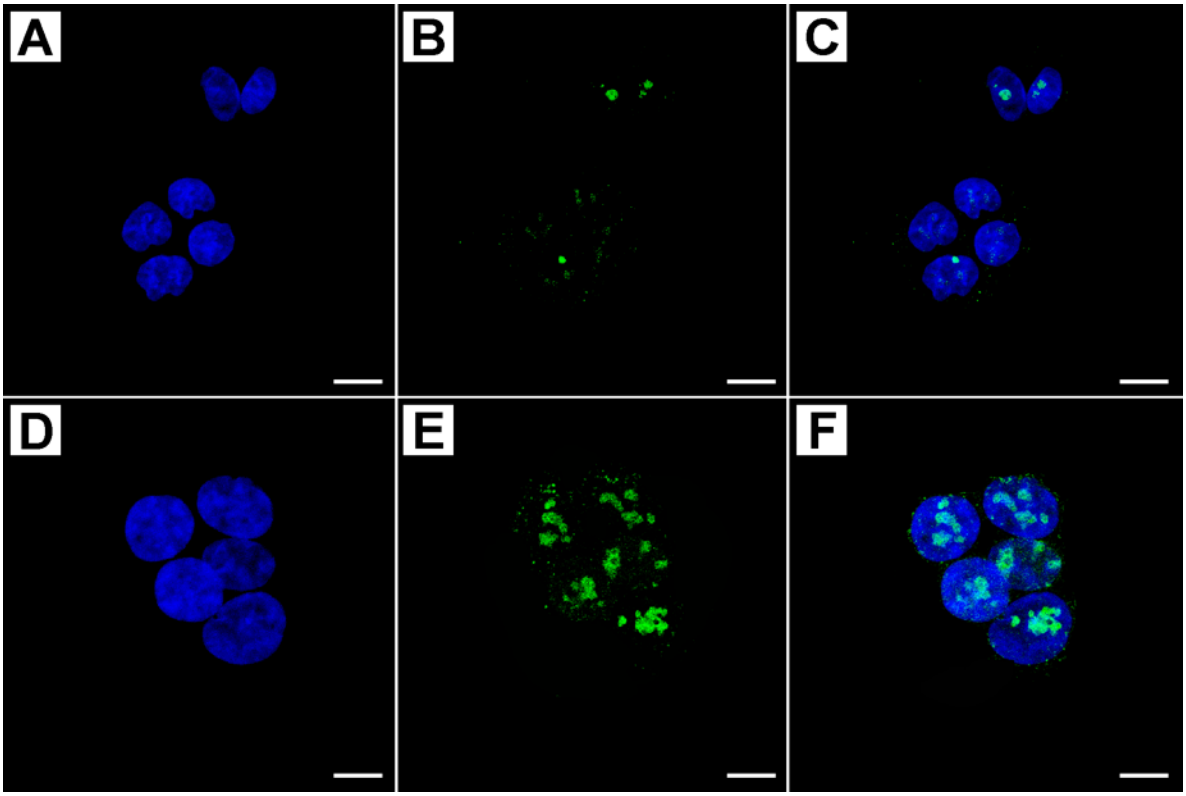

Figure 2. Confocal analysis of Ki-67 protein in treated and untreated cells with graded concentrations of metformin (blue: DAPI; green: Ki-67; C,F: merge). **(A–C)** Cells treated with 10 mM metformin (MET) for 48 h showed weak immunostaining at the nuclear level, whereas **(D–F)** untreated cells were very marked. Scale bar = 8 μm.

Treatment with metformin (MET) 50 mM for 48 h caused a maximum decrease of 45% in the proliferation index, as reported in Table 1, which collects data of semiquantitative evaluation of immunostaining intensity (immunofluorescence intensity score, IFIS).

Furthermore, immunofluorescence analysis was conducted using apoptotic- and autophagic-specific markers in order to determine whether the inhibitory effect of metformin on colorectal cancer cells triggered programmed cell death or autophagy.

Using these techniques, we evaluated both qualitatively and quantitatively cleaved PARP-1, apoptosis-activating factor-1 (APAF-1), caspase-3, and MAP LC3 protein expression. Figure 3 shows the co-immunostaining of cleaved PARP-1 and caspase-3.

Peer-reviewed version available at Int. J. Mol. Sci. 2018, 19, 1478; doi:10.3390/ijms19051478

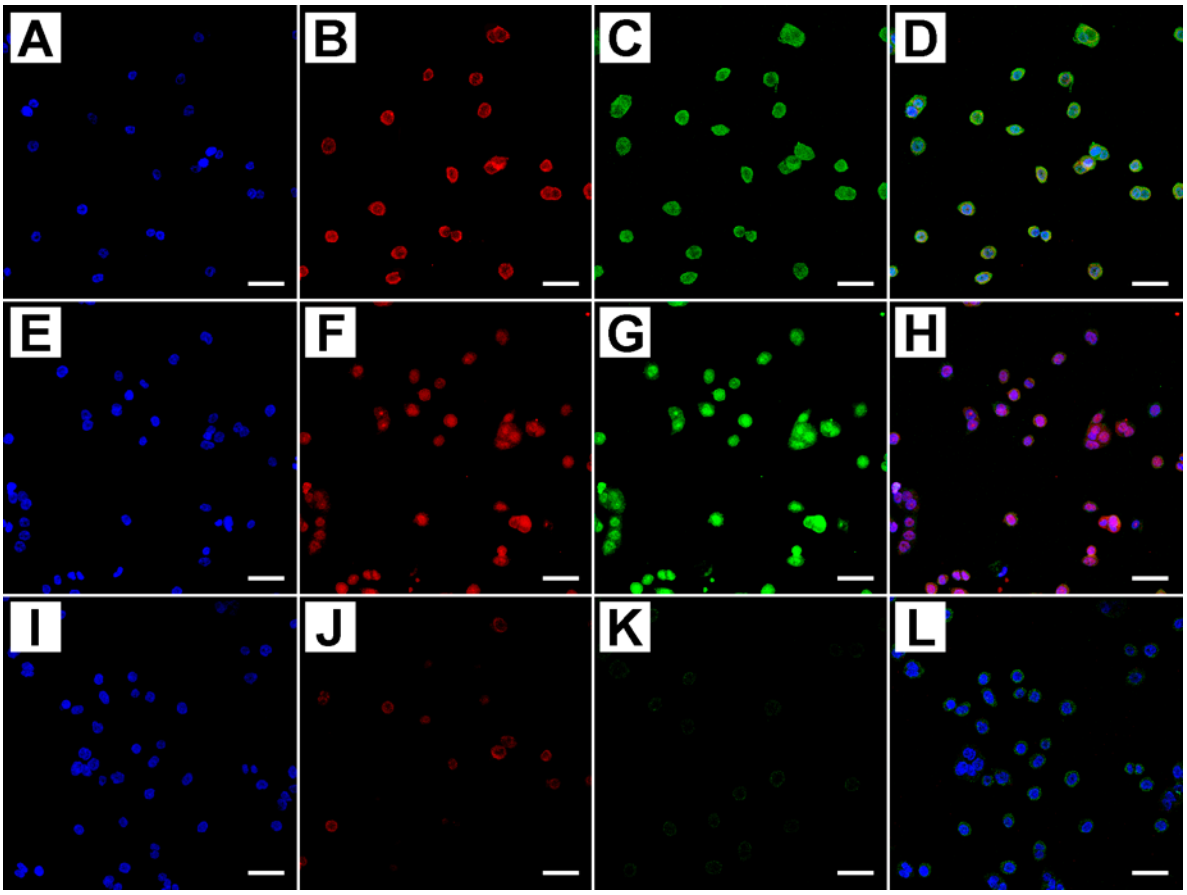

Figure 3. Confocal analysis of cleaved PARP-1 and caspase-3 active proteins in treated and untreated cells with different concentrations of metformin (blue: DAPI; red: cleaved PARP-1; green: caspase-3 active; D,H,L: merge). **(A–D)** Cells treated with 10 mM MET for 24 h showed strong immunostaining for both proteins, as did **(E–H)** cells treated with 25 mM MET for 24 h. **(I–L)** Untreated cells showed a significant decrease in cleaved PARP-1 and caspase-3 active protein expression. Scale bar = 15 μm.

Cleaved PARP-1 antibody detects endogenous levels of the large fragment (89 KDa) of the human protein resulting from cleavage of the native protein and does not recognize the full-length PARP-1 or other isoforms. Cleaved PARP-1 was detectable in the nucleus of treated HT-29 cells, but was not appreciable in untreated cells (Figure 3K). Some representative staining patterns are shown in Figures 3A–D, where nuclear labelling of apoptotic cells is evident, as revealed by DAPI staining. Caspase-3 was aggregated in small clumps distributed in the cytoplasm of cultured treated cells, and both proteins showed an increased expression pattern related to the dose and time of metformin treatment, as shown in Figures 3A–H. Untreated cells were negative for immunostaining (Figures 3I–L).

Figure 4 shows the immunostaining of APAF-1 and MAP LC3.

Peer-reviewed version available at Int. J. Mol. Sci. 2018, 19, 1478; doi:10.3390/ijms19051478

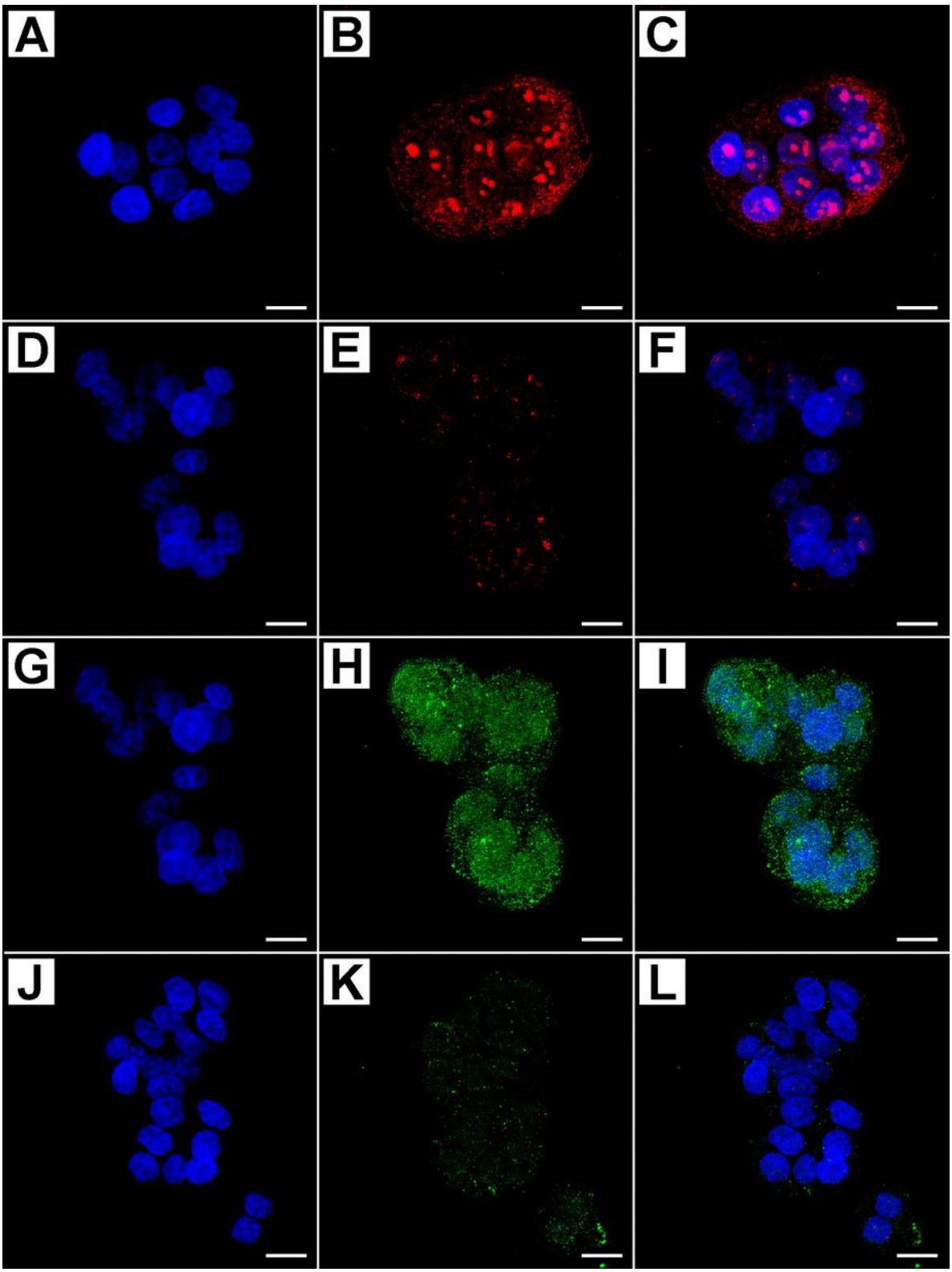

Figure 4. Confocal analysis of apoptosis-activating factor-1 (APAF-1) and MAP LC3 proteins in treated and untreated cells with different concentrations of metformin (blue: DAPI; green: MAP LC3; red: APAF-1; C,F,I,L: merge). **(A–C)** In cells treated with 50 mM MET for 48 h, APAF-1 show a diffuse or granular staining pattern at the nuclear level, while in **(D–F)** untreated cells, nuclear expression is barely detectable. **(G–I)** In cells treated with 50 mM MET for 48 h, MAP LC3 protein shows two distinct autophagic patterns: a diffuse, finely granular reactivity dispersed in the cytoplasm, and a rounded, densely stained material, probably enclosed within a cytoplasmic vacuole that accumulates prevalently around the nucleus; **(J–L)** untreated cells were very weakly marked. Scale bar = 10 μm.

Peer-reviewed version available at Int. J. Mol. Sci. 2018, 19, 1478; doi:10.3390/ijms19051478

The staining patterns of the first protein varied from diffuse to granular in the nucleus of treated cells; on the other hand, cells expressing MAP LC3 protein showed two distinct autophagic patterns: a diffuse, finely granular reactivity dispersed in the cytoplasm and a rounded, densely stained material, probably enclosed within a cytoplasmic vacuole that accumulated prevalently around the nucleus (Figures 4G–I).

The dense, rounded autophagic vacuoles were recognizable in cells treated with higher doses and for longer time; such structures varied in size and density, but usually formed coarse, rather than fine, granules. Untreated cells showed weak marking for both proteins (Figures 4D–F, J–L).

The semiquantitative evaluation of immunostaining intensity, reported as immunofluorescence intensity score (IFIS) in Table 1, showed that the level of cleaved PARP-1, caspase-3, APAF-1, and MAP LC3 proteins had an increasing trend in a dose- and time-dependent manner, with statistical significance of the different expressions among the groups of treated cells and with respect to untreated cells.

Table 1: Evaluation of immunostaining intensity (immunofluorescence intensity score, IFIS).

	IFIS (mean ± SD): 24 h				**IFIS (mean ± SD): 48 h**			
	Ctrl	**10 mM**	**25 mM**	**50 mM**	**Ctrl**	**10 mM**	**25 mM**	**50 mM**
Cleaved PARP-1	20.0 ± 4.3	47.0 ± 11.0	63.0 ± 9.8	76.0 ± 15.0	23.0 ± 12.0	55.0 ± 6.7	74.0 ± 13.0	89.0 ± 22.0
Caspase-3	36.0 ± 9.5	49.0 ± 23.0	69.0 ± 15.0	91.0 ± 7.4	32.0 ± 5.7	64.0 ± 17.0	97.0 ± 20.0	101.0 ± 29.0
APAF-1	31.0 ± 7.5	54.0 ± 3.9	66.0 ± 19.0	85.0 ± 9.5	27.0 ± 7.0	72.0 ± 17.0	72.0 ± 17.0	93.0 ± 12.0
MAP LC3	26.0 ±4.7	45.0 ± 7.2	71.0 ± 7.6	93.0 ± 15.0	28.0 ± 8.3	57.0 ± 6.3	84.0 ± 5.4	103.0 ± 32.0
NRF-2	55.0 ± 7.2	43.0 ± 6.3	31.0 ± 4.8	19.0 ± 3.7	63.0 ± 12.0	47.0 ± 5.4	30.0 ± 7.5	23.0 ± 3.0
NF-Kb	60.0 ± 9.5	54.0 ± 8.3	47.0 ± 15.0	32.0 ± 7.4	67.0 ± 5.7	50.0 ± 17.0	33.0 ± 2.0	25.0 ± 2.9

$P < 0.05$ between all group pairs.

To corroborate the findings of the morphological evaluation previously described, cell lysates of cultured treated and untreated cells were subjected to Western blot analysis. As shown in Figure 5, protein bands immunopositive for APAF-1, cleaved PARP-1, MAP LC3, and caspase-3 were clearly evident in treated cells.

Preprints (www.preprints.org) | NOT PEER-REVIEWED | Posted: 21 March 2018 doi:10.20944/preprints201803.0184.v1

Peer-reviewed version available at Int. J. Mol. Sci. 2018, 19, 1478; doi:10.3390/ijms19051478

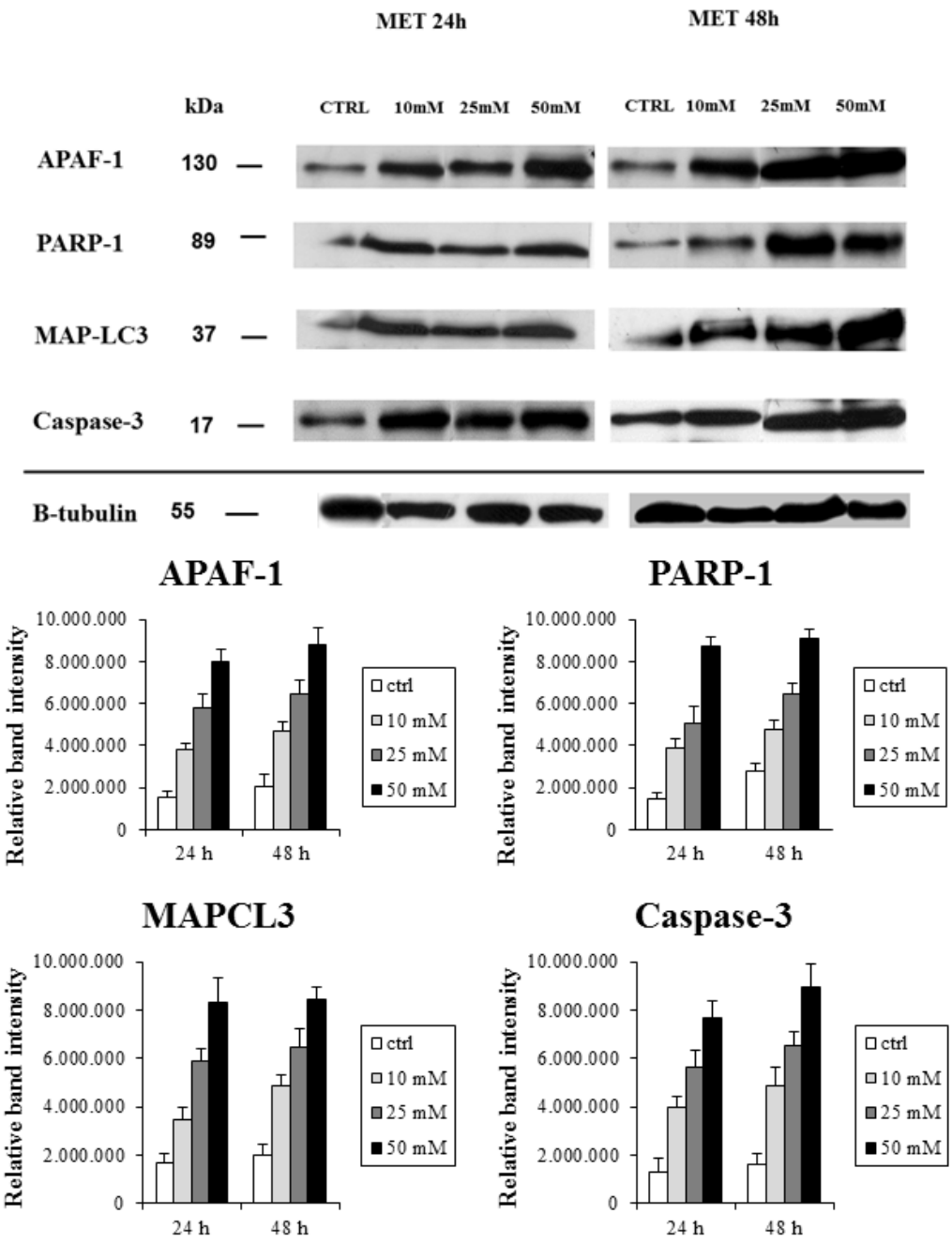

Figure 5. Western blot analysis of HT29 cells treated with graded concentrations of metformin, 10 mM/25 mM/50 mM for 24 h and 48 h, and of untreated cells (Ctrl), using anti-APF-1, cleaved PARP-1, MAP LC3, and caspase-3 antibodies. Mean densitometric data of APAF-1, cleaved PARP-1, MAP LC3, and caspase-3 expressions were analyzed using Image J software. $P < 0.05$ between all group pairs.

Lysates of untreated cells generally yielded only faint bands for all these markers. Densitometric analysis and normalization (with equal amounts of protein loading) of the immunoreactivity signals from protein extracts of treated and untreated cells showed that the expression pattern had an increased trend related to dose and time of treatment. Western blotting and densitometric analysis were performed in triplicate; quantification of protein expressions between different groups of treatment and with respect to the untreated group achieved statistical significance.

2.2 Metformin Alters NRF-2 and NF-κB Expression in HT29 Cells in a Dose- and Time-Dependent Manner

Peer-reviewed version available at Int. J. Mol. Sci. 2018, 19, 1478; doi:10.3390/ijms19051478

Confocal analysis was conducted on HT29 cells treated with increasing amounts of metformin (0, 10, 25, and 50 mmol/L), as described above, to analyze the expression patterns of NRF-2 and NF-κB proteins. The results demonstrate that metformin affects the survival of cultured cells inhibiting the transcriptional activation of NRF-2 and NF-κB. In Figures 6A–C, the presence of NRF-2 at the nuclear level in untreated cells is clearly evident, as a consequence of the translocation of the transcriptional factor into the nucleus; in particular, nucleolar domains appeared strongly marked (Figure 6B).

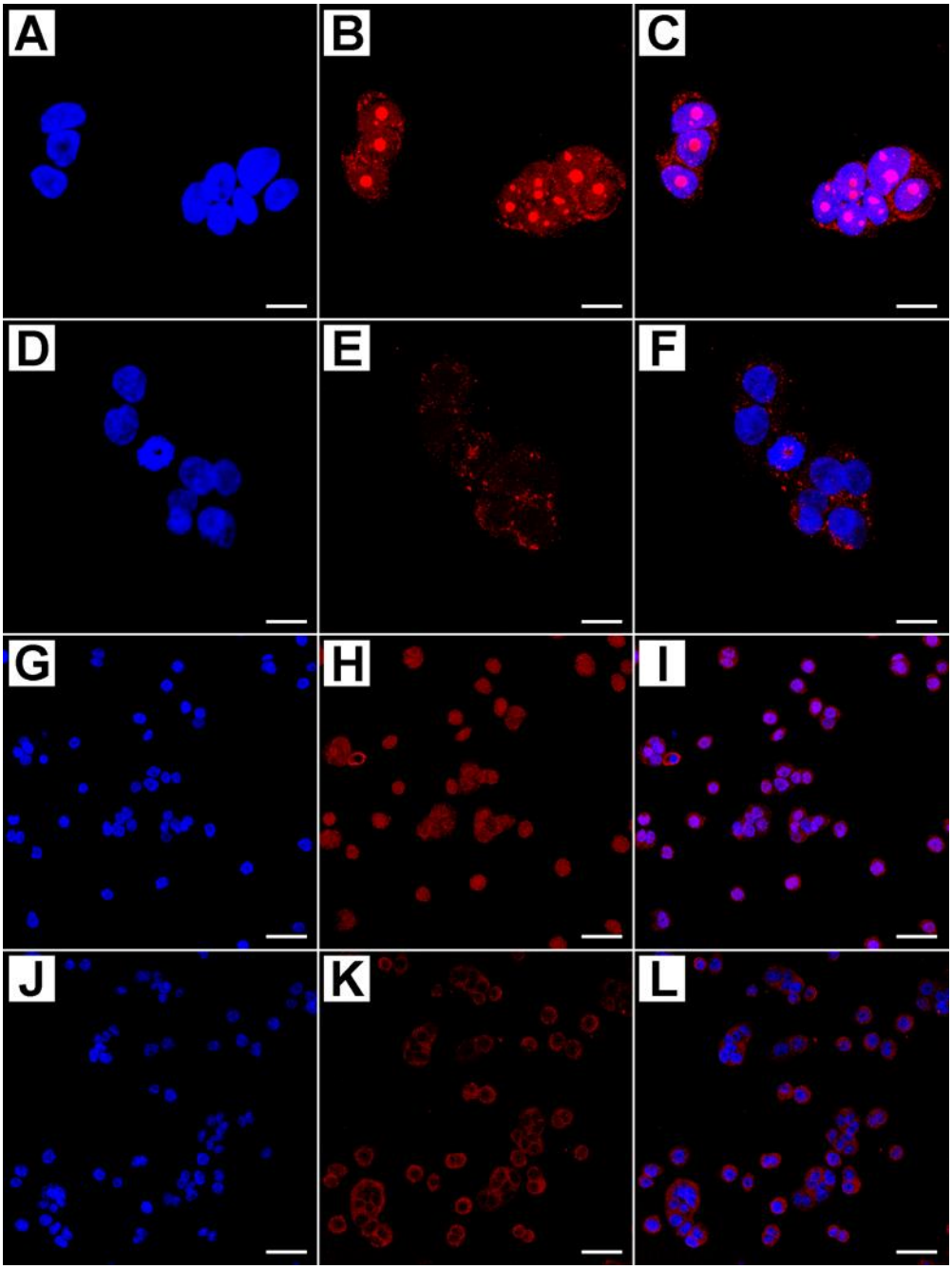

Figure 6. Confocal analysis of NRF-2 and NF-κB proteins in treated and untreated cells with graded concentrations of metformin (blue: DAPI; red: NRF-2 and NF-κB; C,F,I,L: merge). **(A–C)** NRF-2 clearly showed strong nuclear reactivity in untreated cells, whereas **(D–F)** in cells treated with 25 mM MET for 24 h, the reactivity was finely dispersed only in the cytoplasmic compartment. **(G–I)** NF-κB showed significant translocation into the nucleus of untreated cells with 25 mM MET for 24 h, while **(J–L)** in treated cells, the protein was scattered in the cytoplasm. Scale bar = 10 μm.

Preprints (www.preprints.org) | NOT PEER-REVIEWED | Posted: 21 March 2018 doi:10.20944/preprints201803.0184.v1

Peer-reviewed version available at Int. J. Mol. Sci. 2018, 19, 1478; doi:10.3390/ijms19051478

Treated cells showed a detectable presence of this protein in the cytoplasm, while the nuclei were slightly marked (Figures 6D–F). The effects of metformin on HT29 cells is dose-dependent and time-dependent, because there was a significant change in the parameters analyzed after 48 h of treatment compared to 24 h (Table 1).

NF-κB protein showed very intense immunostaining in the nuclear compartment in untreated samples, while the cytoplasm was less stained (Figures 6G–I). In treated cells, the presence of this protein was appreciable only in the cytoplasmic compartment and the staining was evenly distributed throughout the cell (Figures 6J–L). Semiquantitative evaluation of immunostaining intensity (IFIS) in Table 1 showed that the level of NRF-2 and NF-κB proteins had a decreasing trend in a dose- and time- dependent manner, with statistical significance of the different expressions among the groups of treated cells and with respect to the untreated ones.

Western blot analysis showed that NRF-2 expression decreased after treatment with increasing concentrations of metformin. This observation was more evident after 48 h of treatment. The expression pattern of NF-κB was slightly different; the protein amount decreased with higher doses of metformin with respect to NRF-2 (Figure 7).

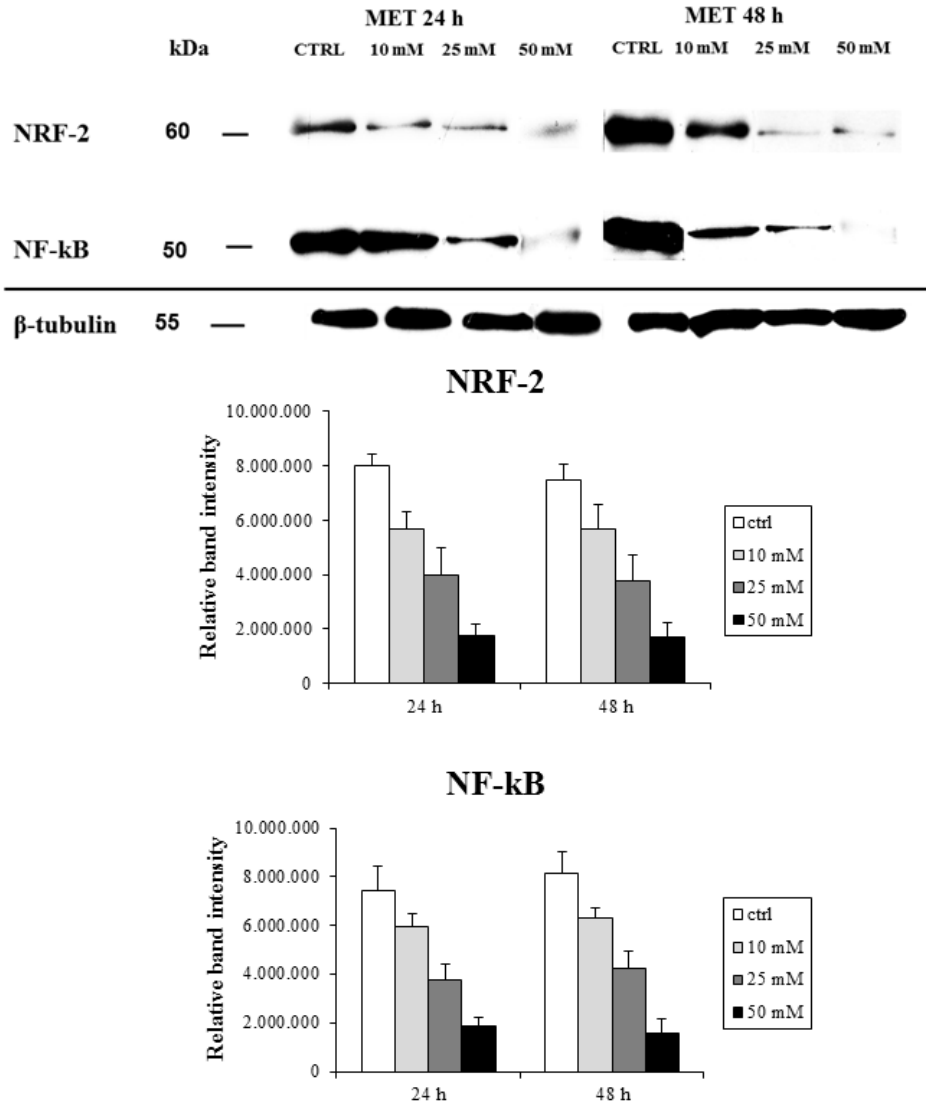

Figure 7. Western blot analysis of HT29 cells treated with graded concentrations of metformin, 10m M/25 mM/50 mM, for 24 h and 48 h and of untreated cells (Ctrl), using anti–NRF-2 and anti–NF-κB

antibodies. Mean densitometric data of NRF-2 and NF-κB expressions were analyzed using Image J software. P <0.05 between all group pairs.

Densitometric analysis and normalization (with equal amounts of protein loading) of the immunoreactivity signals from protein extracts of treated and untreated cells showed that the expression pattern had a decreased trend related to dose and time of treatment. Western blotting and densitometric analysis were performed in triplicate; quantification of protein expressions between different treatment groups and with respect to the untreated group achieved statistical significance.

2.3 Flow Cytometry Analysis Demonstrates that Metformin Exerts an Inhibitory Effect on HT29 Cell Survival

The ability of metformin treatment to induce apoptosis in HT-29 cells was determined using an Annexin V-FITC assay to establish the relationship between antiproliferation and apoptosis.

Staining with fluorescein isothiocyanate (FITC), Annexin V clearly showed that the percentage of apoptotic HT29 cells treated with metformin increased in a time- and dose-dependent manner when comparing treatments to each other. Similarly, the early apoptotic death rate of the HT29 cells treated with MET was remarkably higher than that of the controls (Figures 8A,B). The highest rate of cell apoptosis (60%) was achieved with the 50 mM treatment for 48 h (Figure 8B). Flow cytometry analyses were performed in triplicate and the results, which reached statistical significance, agreed with those obtained by confocal microscopy analysis and Western blot experiments.

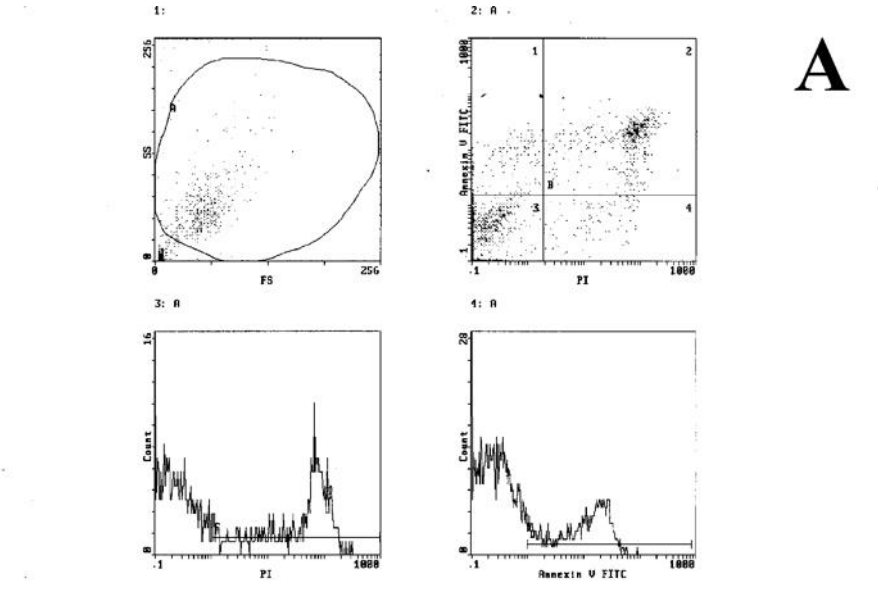

Stats: Not Normalized, Listgating: Disabled

Hist	Region	ID	%	Count	Mn X	Mn Y	PkPosX	PkPosY	PkCnt	FPCVX	FPCVY
1	A	A	57.5	6182	56.0	63.1	48.0	46.0	11	40.18	46.18
2	B1	B	5.10	315	0.449	6.20	0.102	1.58	6	94.72	81.31
	B2	B	15.5	958	46.6	14.2	82.5	28.0	8	125.25	86.38
	B3	B	76.0	4698	0.121	0.176	0.102	0.102	2164	43.79	70.88
	B4	B	3.41	211	17.3	0.594	71.5	0.768	3	115.14	74.52

Hist	Region	ID	%	Count	Mn X	Md X	PkPosX	PkCnt	HPCV	Min	Max
3	C	C	20.3	1256	31.9	60.6	68.9	15	1.11	1.10	1024
4	D	D	23.0	1423	9.42	12.5	17.7	12	0.71	1.02	878.8

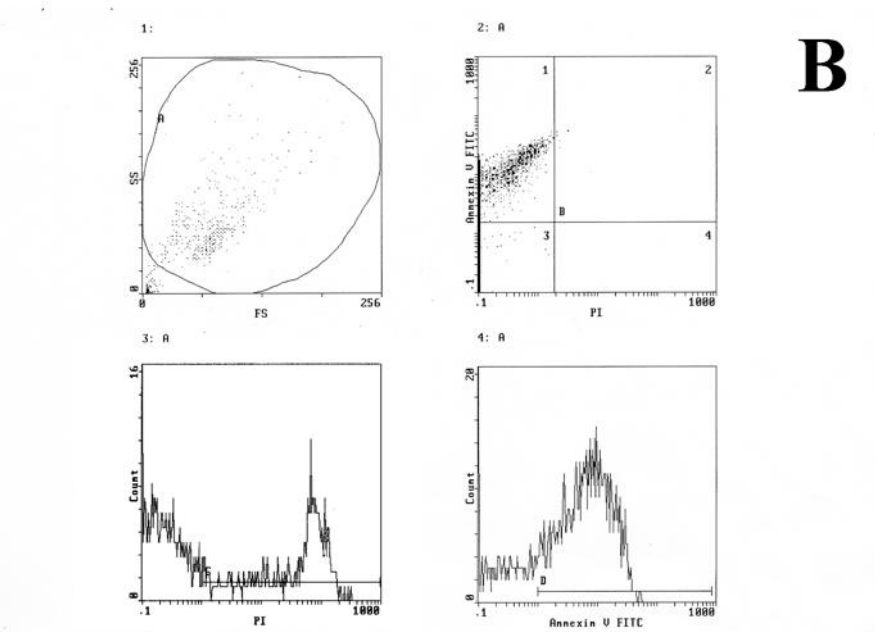

Stats: Not Normalized, Listgating: Disabled

Hist	Region	ID	%	Count	Mn X	Mn Y	PkPosX	PkPosY	PkCnt	FPCVX	FPCVY
1	A	A	79.3	4830	76.1	76.6	72.0	59.0	8	42.57	46.30
2	B1	B	59.9	2895	0.207	7.51	0.102	4.32	70	84.87	83.15
	B2	B	0.29	14	2.58	37.0	3.24	53.6	2	24.52	52.46
	B3	B	39.8	1921	0.105	0.204	0.102	0.102	1036	19.83	94.64
	B4	B	0.00	0	****	****	****	****	**	**	**

Hist	Region	ID	%	Count	Mn X	Md X	PkPosX	PkCnt	HPCV	Min	Max
3	C	C	2.63	127	1.45	1.33	1.24	7	0.71	1.10	1024
4	D	D	64.5	3116	6.92	7.36	9.88	19	2.06	1.02	878.8

Figure 8. Flow cytometry analysis of (**A**) untreated and (**B**) treated cells with graded concentrations of metformin, using an Annexin V-FITC (fluorescein isothiocyanate) assay. (**A**) The early apoptotic death rate of untreated HT29 cells was 5.1% (line 2, third column of the table below the figure). (**B**) The early apoptotic death rate of the HT29 cells treated with MET was remarkably higher than that of the control. The highest rate of cell apoptosis, 59.9%, was achieved with the 50 mM treatment for 48 h (line 2, third column of the table below the figure).

3. Discussion

In this study, HT29 cells were treated with different concentrations of metformin, 10 mM/25 mM/50 mM, for 24 and 48 hours. We performed immunofluorescence experiments by means of confocal microscopy and Western blot analysis to evaluate a panel of factors involved in apoptotic/autophagic processes and oxidative stress response. Moreover, HT29 cells treated with metformin were analyzed by flow cytometry assay to detect the apoptotic rate of the cells. The first observations concern the phenotype of HT29 cells treated with metformin, which showed modifications of cell morphology, probably due to the partial loss of plasma membrane attachment; these features are characteristic of the earliest phases of the apoptotic process. The immunofluorescence analysis of Ki-67 expression pattern corroborates this finding; in fact, there was a strong decrease of Ki-67 protein in treated cells with respect to the untreated ones. All these results were related to dose and time of treatment. Moreover, the apoptosis-inducing activity of metformin causes an increase in the early apoptotic death rate, which results in poor survival of cells after treatment, as clearly demonstrated by flow cytometry experiments. Overall, these results show that metformin could not only inhibit the growth of HT29 cells, but also induce cell apoptosis. These considerations were supported by the analysis of key factors involved in the apoptotic process as APAF-1, cleaved PARP-1, and active caspase-3. Cell apoptosis is activated in response to both intrinsic and extrinsic pathways. Drug therapies that induce apoptosis cause DNA damage–induced and p53-regulated release of cytochrome-c from mitochondria. Cytochrome-c, in turn, binds to apoptosis-activating factor-1 (APAF-1), resulting in activation of caspase-9, which is followed by the activation of effector caspases including caspase-3. Following ligation, death receptors signal cell death by inducing a death-inducing signaling complex composed of the cytoplasmic adapter protein Fas-associated death domain and caspase-8. Activated caspase-8 can activate caspase-3 both directly and indirectly by truncation of Bid [21]. Metformin has been shown to induce cancer cell apoptosis through both the intrinsic and extrinsic pathways [22]. In this study, we observed that increased active caspase-3, cleaved PARP-1, and APAF-1 expressions were higher in treated cells with respect to untreated cells in a statistically significant manner in the lowest metformin concentration used (10 mMol/L). Previously, metformin at 20 mmol/L was shown to be effective against breast cancer [23], melanoma [24], and gastric cancer [25]. The concentration of metformin administered to type 2 diabetic patients is approximately 30–60 μmol/L [26]. Thus, the doses of metformin that were shown to be effective against cancer cells are approximately 300 to 600–fold (around 20 mmol/L) greater than the dose routinely administered for diabetic disorders. In this study, we also used a low dose of metformin (10 mmol/L) in order to establish whether the drug induces apoptosis at doses that avoid toxic side effects to cells. The results confirm that metformin was effective even at low doses, and higher metformin concentrations led to an increased rate of apoptosis. Similarly, elevated levels of autophagic marker expression were observed in treated cells. This result may have controversial interpretations; in fact, recent studies suggest that autophagy plays a dual role in determining cell fate, which means that it could be a survival mechanism or induce programmed cell death, depending on different cellular stresses. In some conditions, the activation of autophagy provides cell protection, presumably by eliminating dysfunctional organelles and proteins and maintaining the energy balance. To a large extent, the cytoprotective function of autophagy appears to be a consequence of autophagy induction inhibiting apoptosis through a crosstalk between autophagy and apoptosis regulatory pathways. On the other hand, autophagy is also considered a type of cell death program [27]. It is well known that there are three types of cell death. Necrosis, a type of unprogrammed cell death, evokes a cellular inflammation reaction by immunological activation and subsequently leads to cell death in neighboring cells. Apoptosis, which is programmed cell death type I, is characterized by the formation of chromatin condensation, DNA fragmentation, and apoptotic bodies. Cell death by overactivated autophagy has been referred to as programmed cell death type II [28]. Upregulation of autophagy has been shown to lead to cell death in order to eliminate damaged or abnormal cells. It would seem reasonable to expect that cytotoxic autophagy should be a consequence of higher levels or a more prolonged process of cellular self-digestion rather than of cytoprotective autophagy. However, there is no explicit experimental evidence suggesting

Peer-reviewed version available at Int. J. Mol. Sci. 2018, 19, 1478; doi:10.3390/ijms19051478

that cytotoxic autophagy is uniquely different from cytoprotective autophagy. In general, depending on the type of the tumor and stimuli, as well as the extent of DNA damage, autophagy can have both cytoprotective and cytotoxic functions [29].

Another point to be discussed is the response of NRF-2 protein to metformin treatment; the NRF-2 expression profile is negatively regulated by the drug in a dose- and time-dependent manner. This finding is very intriguing, as there is research aimed at defining the boundaries between NRF-2 positive and negative effects in cancer and establishing a precise rationale for undertaking NRF-2 therapeutic targeting. The main function of the transcription factor NRF-2 is to activate the cellular antioxidant response by inducing the transcription of several genes to protect cells from the effects of exogenous and endogenous insults such as xenobiotics and oxidative stress [30]. As a result, NRF-2 has typically been regarded as a cytoprotective transcription factor and is considered as the main defense mechanism of the cell and a major regulator of cell survival. Thus, NRF-2 has been traditionally deemed to be a tumor suppressor. Indeed, NRF-2–deficient mice are more sensitive to carcinogenesis [31,32], and NRF-2 loss has been linked to enhanced metastatic potential [33,34]. However, in the past few years increasing evidence suggests that NRF-2 activation might not be beneficial in all cancer types and stages. In fact, NRF-2 promotes survival not only of normal cells, but also of cancer cells, supporting the hypothesis that NRF-2 activation in malignant cells might sustain the evolution of the disease. The identification of a "dark side" of NRF-2 [35,36] has generated controversy, because it is still unclear whether NRF-2 acts as a tumor suppressor or as an oncogene [35,37]. Indeed, since oxidative stress is involved in the initiation of cancer, the antioxidative function of NRF-2 may play an anticancer role and may be useful in cancer chemoprevention. NRF-2 hyperactivation in tumors creates an environment that may favor the survival of cancer cells by protecting them from excessive oxidative stress, chemotherapeutic agents, or radiotherapy [30,38,39]. Indeed, in human tumor samples and cell lines, constitutive NRF-2 activation increases the expression of some genes involved in drug metabolism, thereby sustaining resistance to chemotherapeutic drugs and radiotherapy [40]. NRF-2 can play an important role in chemoresistance, preventing the intracellular accumulation of drugs in cancer cells and subsequently protecting cells from apoptosis [41]. These literature data are in line with our observation that metformin induces an increase of apoptotic key factors and reduces the nuclear translocation of NRF-2 protein. To our knowledge, this is the first study to investigate the effect of metformin on NRF-2 protein, and it may provide an opportunity to study new molecules capable of interfering with binding and activation of the NRF-2 pathway. Moreover, the NF-κB expression pattern is drastically affected by metformin treatment; in fact, treated cells showed a significant decrease of NF-κB protein levels. In addition, the protein was present only in the cytoplasmic compartment, whereas in untreated cells NF-κB was expressed at the nuclear level. Several lines of evidence have shown that the transcription factor nuclear factor–kappa B (NF-κB) is a critical determinant, as it regulates a variety of pathophysiological processes, such as inflammation, cell survival, proliferation, invasion, apoptosis, differentiation, and chemoresistance, in different tumor cells, including colorectal cancer [42,43]. Therefore, pharmacologically safe antitumor agents with the potential to influence the tumor microenvironment and inhibit NF-κB signaling activation may enhance chemosensitivity and reduce metastasis of tumor cells, thus providing a promising approach for the prevention or treatment of tumors. Moreover, several studies are posing NF-κB as a key regulator in the crosstalk among the pathways leading to type 2 diabetes mellitus, inflammatory bowel disease, and colorectal cancer [44]. Actually, various carcinogens, growth factors, and inflammatory stimuli, including microbiota and pro-oxidants, activate the transcription factor NF-κB, which plays a central role in inflammation and is mostly expressed in cancers [45]. NF-κB plays a pivotal role in linking chronic inflammation to cancer development through its ability to upregulate several inflammatory and tumor-promoting cytokines such as IL-6, IL-1α, and TNF-α, as well as survival genes such as *BCL2* and *BCLXL* [46]. In addition, NF-κB promotes EMT, through its activation of snail and twist [47] in the microenvironment, and the expression of inflammatory cytokines. Moreover, NF-κB seems to be involved in tumor-associated macrophage recruitment and acts in cancer-associated fibroblasts by promoting the expression of a proinflammatory gene signature, which is important for macrophage

Peer-reviewed version available at Int. J. Mol. Sci. 2018, 19, 1478; doi:10.3390/ijms19051478

recruitment, neovascularization, and tumor growth, which are abolished when NF-κB is inhibited [48]. This study shows that metformin has an antiproliferative effect related to changes in the expression of the NRF-2/NF-κB pathways, as well as an apoptotic effect on human colon cancer cells. Although further studies are needed to elucidate the detailed correlation between these processes, it can be hypothesized that metformin, already widely used in humans as antidiabetic drug, might be a promising candidate for the prevention or treatment of colorectal cancer. On the other hand, type 2 diabetes mellitus, colorectal cancer, and inflammatory bowel disease are commonly occurring, interrelated clinical problems. They share a common basis influenced by disease-related inflammation, a process characterized by upregulation of expression of common inflammatory cytokines along with TGFβ, TNFα, NF-κB, reactive oxygen species, and other signaling molecules, leading to an imbalance in the intestinal microbiota. The intersection and converging of all these molecular pathways constitute a crosstalk, which affects the pathogenesis of the above-mentioned chronic diseases. A treatment that can interfere with this crosstalk could be a novel therapeutic target of interest in managing the three diseases.

4. Materials and Methods

4.1 Cell Culture

The human colon carcinoma cell line HT29 was obtained from the American Type Culture Collection and grown in Dulbecco's modified Eagle's medium supplemented with 10% fetal bovine serum, glutamine (4 mM), and penicillin (100 U/ml)/streptomycin (100 g/ml). Cell cultures were maintained at 37 °C in 5% CO_2 and 95% air. HT29 cells were plated at the approximate density of 1×10^6 cells/dish in 10 cm^2 culture dishes, 4×10^4 cells/well in 2-well chamber glass slides, and 1×10^4 cell/well in 96-well tissue culture plates. When cells reached approximately 60% confluence, the medium was replaced with serum-free cell medium containing different concentrations of metformin (0, 10, 25, and 50 mmol/L) and the cells were cultured for 24 and 48 h at 37 °C in 5% CO_2 and 95% air. The cells were trypsinized with 0.25% trypsin and 0.2 g/L EDTA and harvested for further studies. Metformin was purchased from Sigma Aldrich (PHR 1084) and was dissolved in sterile water at a stock dose of 1 M for further application.

4.2 Cell Counting

Cells were seeded at a density of 20,000/well and counted at day 1, 2, and 3 after plating. For counting, cells were detached from the wells by washing in a solution of 0.25% trypsin and 0.2 g/L EDTA. Thereafter, 1 ml normal culture medium was added to stop the trypsinization; a 500 µl cell suspension, to which 70 µl trypan blue was added, was transferred to a Burker chamber for cell counting. The number of cells, expressed as number/ml, was determined by 2 blinded observers.

4.3 Western Blot Analysis

Whole cell lysates were obtained from cultured cells, as described above, and extracted with hypotonic buffer (50 mM Tris-Cl, pH 7.8, containing 1% Nonidet P40, 140 mM NaCl, 0.1% SDS, 0.1% Na deoxycholate, 1 mM Na3VO4, and freshly added protease inhibitor cocktail). Lysates were then cleared by centrifugation for 15 min in a refrigerated centrifuge at maximum speed, and immediately boiled in SDS sample buffer. An amount of 40 mg of protein extract from each treatment condition was electrophoresed on SDS-PAGE and transferred to nitrocellulose membranes. The membranes were blocked with 3% dry milk and 2% BSA in phosphate-buffered saline with Tween (PBS-T), and incubated with the following antibodies (diluted 1:1000 overnight at 4 °C under agitation): mouse anti-human APAF-1, rabbit anti-human MAP LC3, mouse anti-human NF-κB (Santa Cruz); mouse anti-human cleaved PARP-1 (Cell Signaling); mouse anti-human NRF-2 (Abcam), mouse anti-human Ki-67 (DAKO). After washing, the membranes were incubated with secondary HPR-conjugated goat anti-mouse IgG antibody (1:5000) or HPR-conjugated goat anti-rabbit IgG antibody (1:5000) (Thermo Scientific) for 30 min at room temperature. Immunoreactive proteins were detected with ECL (Amersham). Anti-mouse-β tubulin (Sigma Aldrich) was used as loading control. Densitometry

Peer-reviewed version available at Int. J. Mol. Sci. 2018, 19, 1478; doi:10.3390/ijms19051478

analysis was performed using a Kodak (Rochester, NY) Image Station 440 cf system, and semiquantitative analysis was performed with Image J software (National Institutes of Health). For each sample and marker, the band intensities were normalized to β-tubulin, and results are expressed as the normalized treatment-to-control ratio.

4.4 Evaluation of Immunofluorescence by Confocal Microscopy

Cells cultured in 2-well chamber glass slides were used for immunofluorescence analysis to evaluate the expression of MAP LC3, APAF-1, cleaved PARP-1, NRF-2, NF-κB, and Ki-67 proteins. Monolayered cells were fixed in 4% paraformaldehyde in PBS for 10 min. After treatment with 3% BSA in PBS for 30 min at room temperature, they were incubated with the primary antibodies (mouse anti-human APAF-1, rabbit anti-human MAP LC3, mouse anti-human active caspase-3, mouse anti-human NF-κB, Santa Cruz; mouse anti-human cleaved PARP-1, mouse anti-human NRF-2, Abcam; mouse anti-human Ki-67, DAKO), diluted 1:25 in PBS containing 3% BSA for 1 h at room temperature. After washing in PBS, the samples were incubated for 1 h at room temperature with the secondary antibodies diluted 1:20 in PBS containing 3% BSA (sheep anti-mouse FITC conjugated, goat anti-rabbit TRITC conjugated, Sigma Aldrich). After washing in PBS and H_2O, the samples were counterstained with 1mg/ml DAPI in H_2O and then mounted with antifading medium (0.21 M DABCO and 90% glycerol in 0.02 M Tris, pH 8.0). Negative control samples were not incubated with the primary antibody. Confocal imaging was performed under a Leica TCS SP2 AOBS confocal laser scanning microscope. Excitation and detection of the samples were carried out in sequential mode to avoid overlapping of signals. Sections were scanned with laser intensity, confocal aperture, gain, and black level setting kept constant for all samples. Optical sections were obtained at increments of 0.3 mm in the z-axis and were digitized with a scanning mode format of 512 × 512 or 1024 × 1024 pixels and 256 gray levels. The confocal serial sections were processed with the Leica LCS software to obtain 3-dimensional projections. Image rendering was performed with Adobe Photoshop software. The original green fluorescent confocal images were converted to gray-scale and median filtering was applied. An intensity value ranging from 0 (black) to 255 (white) was assigned to each pixel. Background fluorescence was subtracted and immunofluorescence intensity (IF) was calculated as the average for each selected area. The fluorescence intensity at the selected areas, linearly correlated with the number of pixels, was quantitatively analyzed using the standard imaging analysis software of an NIS-Elements system. Each sample was assigned a code number, and the score, referred to as immunofluorescence intensity score (IFIS), was determined by an observer who was blind to tissue groups during the analysis [49].

4.5 Flow Cytometry Analysis

The apoptotic status of HT29 cells was evaluated by measuring the exposure of phosphatidylserine on the cell membranes using Annexin V-FITC (fluorescein isothiocyanate) and propidium iodide (PI) staining [50]. The BD Pharmingen Annexin V-FITC Apoptosis Detection Kit I (BD Biosciences, Franklin Lakes, NJ, USA) was used for the apoptosis assay. HT29 cells were plated in a 24-well plate (1 × 106 cells ml-1), and after 24 h incubation, the cells were treated with graded concentrations of metformin (0, 10, 25, and 50 mmol/L) for 24 and 48 h and harvested. After centrifugation, the cell pellets were washed twice with cold phosphate-buffered saline (137 mM NaCl, 2.7 mM KCl, 10 mM Na2HPO4, pH 7.4) and suspended in 100 µl of 1× binding buffer (10 mM Hepes/NaOH, 140 mM NaCl, 2.5 mM CaCl2, pH 7.4). The cells were incubated with 5 µl Annexin V-FITC and 10 µl PI at room temperature for 15 min in the dark. After incubation, 400 µl of 1× binding buffer was added to each tube. The cells were analyzed immediately by Epics XL-MCL Flow Cytometry (Beckman Coulter, Italy).

4.6 Statistical Analysis

All experiments were performed in triplicate. Data are expressed as means ± standard deviation. Statistical comparisons of results were made using analysis of variance. Significant differences ($p < 0.05$) between the means of control and metformin-treated cells were analyzed by Student's t-test.

Acknowledgments: The study was supported by funds from the Associazione per la Ricerca sui Tumori Intestinali and Fondazione Cassa di Risparmio di Vignola. The authors wish to thank the Centro Interdipartimentale Grandi Strumenti of the University of Modena and Reggio Emilia for software, instrument availability, and assistance.

Author Contributions: Paola Sena and Luca Roncucci conceived and designed the experiments; Paola Sena and Marta Benincasa performed the experiments; Paola Sena and Stefano Mancini analyzed the data; Carla Palumbo and Francesco Mariani contributed reagents/materials/analysis tools; Paola Sena and Luca Roncucci wrote the paper

Conflicts of Interest: The authors declare that there is no conflict of interest regarding the publication of this paper.

References

1. Siegel RL, Miller KD, Jemal A. Cancer statistics, 2017. *CA Cancer J Clin* **2017**,67,7-30, DOI: 10.3322/caac.21395.
2. Anderson WF, Umar A, Brawley OW. Colorectal carcinoma in black and white race. *Cancer Metastasis Rev* **2003**,22,67–82.
3. Das D, Arber N, Jankowski JA. Chemoprevention of colorectal cancer. *Digestion* **2007**,76,51–67, DOI: 10.1159/000108394.
4. Gupta RA, Dubois RN. Colorectal cancer prevention and treatment by inhibition of cyclooxygenase-2. *Nat Rev Cancer* **2001**,1,11–21.
5. Psaty BM, Furberg CD. COX-2 inhibitors—lessons in drug safety. *N Engl J Med* **2005**,352,1133–5, DOI: 10.1038/35094017.
6. Meyskens FL Jr.McLaren CE, Pelot D, et al .Difluoromethylornithine plus sulindac for the prevention of sporadic colorectal adenomas: a randomized placebo-controlled, double-blind trial. *Cancer Prev Res* **2008**,1,32–8, DOI: 10.1158/1940-6207.
7. Limburg PJ, Anderson KE, Johnson TW,et al. Diabetes mellitus and subsite-specific colorectal cancer risks in the Iowa Women's Health Study. *Cancer Epidemiol Biomarkers Prev* **2005**,14,133–7, DOI: 10.1158/1055-9965.
8. Larsson SC, Giovannucci E, Wolk A. Diabetes and colorectal cancer incidence in the cohort of Swedish men. *Diabetes Care* **2005,**28,1805–7.
9. Giovannucci E, AscherioA, Rimm EB, et al. Physical activity, obesity, and risk for colon cancer and adenoma in men. *Ann Intern Med* **1995,**122,327–34.
10. Frezza EE, Wachtel MS, Chiriva-Internati M. Influence of obesity on the risk of developing colon cancer. *Gut* **2006**,55,285–91, DOI: 10.1136/gut.2005.073163.
11. Witters LA. The blooming of the French lilac. *J Clin Invest* **2001,**108,1105–7, DOI: 10.1172/ JCI14178
12. Bodmer M, Meier C, Krähenbühl S, et al .Metformin, sulfonylureas, or other antidiabetes drugs and the risk of lactic acidosis or hypoglycemia: a nested case-control analysis. *Diabetes Care* **2008**,31,2086–91, DOI:10.2337/dc08-1171.
13. Shaw RJ, Lamina KA, Vasquez D, et al. The kinase LKB1 mediates glucose homeostasis in liver and therapeutic effects of metformin. *Science* **2005**,310,1642–6, DOI: 10.1126/science. 1120781.
14. Libby G, Donnelly LA, Donnan PT, et al. New users of metformin are at low risk of incident cancer: A cohort study among people with type 2 diabetes. *Diabetes Care* **2009**,32,1620–5, DOI: 10.2337/dc08-2175.
15. Currie CJ, Poole CD, Gale EA . The influence of glucose-lowering therapies on cancer risk in type 2 diabetes. *Diabetologia* **2009**,52,1766–77, DOI: 10.1007/s00125-009-1440-6.
16. Alimova IN, Liu B, Fan Z, et al. Metformin inhibits breast cancer cell growth, colony formation and induces cell cycle arrest in vitro. *Cell Cycle* **2009,**8,909–915, DOI: 10.4161/cc. 8.6.7933
17. Ben Sahra I, Laurent K, Loubat A, et al. The antidiabetic drug metformin exerts an antitumoral effect in vitro and in vivo through a decrease of cyclin D1 level. *Oncogene* **2008**,27,3576–3586, DOI: 10.1038/sj.onc.1211024.

18. Hirsch HA, Iliopoulos D, Tsichlis PN, et al. Metformin selectively targets cancer stem cells, and acts together with chemotherapy to block tumor growth and prolong remission. *Cancer Res* **2009,**69,7507–7511, DOI: 10.1158/0008-5472.CAN-09-2994.
19. Song CW, Lee H, Dings RP, et al. Metformin kills and radiosensitizes cancer cells and preferentially kills cancer stem cells. *Sci Rep* **2012,**2, 362, DOI: 10.1038/srep00362.
20. Jurjus A, Eid A, Al Kattar S, et al. Inflammatory bowel disease, colorectal cancer and type 2 diabetes mellitus: The links. *BBA Clin*. **2015,**5,16-24, DOI: 10.1016/j.bbacli.2015.11.002.
21. Oudejans JJ, Muris JJ, Meijer CJ. Inhibition of caspase 9 and not caspase 8 mediated apoptosis may determine clinical response to chemotherapy in primary nodal diffuse large B-cell lymphomas. *Cell Cycle* **2005**,4,526-528, DOI: 10.4161/cc. 4.4.1595.
22. Wang LW, Li ZS, Zou DW, et al. Metformin induces apoptosis of pancreatic cancer cells. *World J Gastroenterol* **2008,**14,7192-7198.
23. Zakikhani M, Dowling R, Fantus IG, et al. Metformin is an AMP kinase-dependent growth inhibitor for breast cancer cells. *Cancer Res* **2006,**66,10269-10273, DOI: 10.1158/0008-5472. CAN-06-1500.
24. Janjetovic K, Harhaji-Trajkovic L, Misirkic-Marjanovic M, et al. In vitro and in vivo anti- melanoma action of metformin. *Eur J Pharmacol* **2011**,668,373-382 DOI:10.1016/j.ejphar.2011.07.004
25. Kato K, Gong J, Iwama H, et al. The antidiabetic drug metformin inhibits gastric cancer cell proliferation in vitro and in vivo. *Mol Cancer Ther* **2012,**11,549-560, DOI: 10.1158/1535-7163. MCT-11-0594.
26. Martin-Castillo B, Vazquez-Martin A, Oliveras-Ferraros C, et al. Metformin and cancer: doses, mechanisms and the dandelion and hormetic phenomena. *Cell Cycle* **2010**,9,1057-1064, DOI: 10.4161/cc. 9.6.10994.
27. Russo M, Russo GL. Authopagy inducers in cancer**.** *Biochem Pharmacol***.** 2018, S0006-2952(18)30064-9, DOI: 10.1016/j.bcp.2018.02.007
28. Claude-Taupin A, Jia J, Mudd M, Deretic, V Autophagy's secret life: secretion instead of degradation. *Essays Biochem*, 2017, 12;61(6),637-647. DOI: 10.1042/EBC20170024.
29. Mathew R, Karantza-Wadsworth V, White E: Role of autophagy in cancer. *Nat Rev Cancer* **2007**,7(12),961-967, DOI: 10.1038/nrc2254.
30. Motohashi H, and Yamamoto M. Nrf2–Keap1 defines a physiologically important stress response mechanism. *Trends Mol Med* **2004**,10,549–557, DOI: 10.1016/j.molmed. 2004.09.003.
31. Ramos-Gomez M, Dolan PM, Itoh K, et al. Interactive effects of Nrf2 geno-type and oltipraz on benzo[a]pyrene-DNA adducts and tumor yield in mice. *Carcinogenesis* **2003**,24,461–467.
32. Iida K, Itoh K, Kumagai Y, et al. Nrf2 is essential for the chemopreventive efficacy of oltipraz against urinary bladder carcinogenesis. *Cancer Res* **2004,**64,6424–6431, DOI: 10.1158/0008-5472. CAN-04-1906.
33. Satoh H, Moriguchi T, Taguchi K, et al. Nrf2-deficiency creates a responsive microenvironment for metastasis to the lung. *Carcinogenesis* **2010**;31:1833–1843, DOI: 10.1093/carcin/bgq105.
34. Rachakonda G, Sekhar KR, Jowhar D, et al. Increased cell migration and plas-ticity in Nrf2-deficient cancer cell lines. *Oncogene* **2010,**29,3703–3714, DOI: 10.1038/onc.2010.118.
35. Lau A, Villeneuve NF, Sun Z, et al. Dual roles of Nrf2 in cancer. *Pharmacol Res* **2008**, 58,262–270, DOI: 10.1016/j.phrs.2008.09.003.
36. Wang X J, Sun Z, Villeneuve NF, et al. Nrf2 enhances resistance of cancer cells to chemotherapeutic drugs, the dark side of Nrf2. *Carcinogenesis* **2008,**29,1235–1243, DOI:10.1093/carcin/bgn095.
37. Sporn M B and Liby K T. NRF2 and cancer: the good, the bad and the importance of context. *Nat Rev Cancer* **2012,**12,564–571, DOI: 10.1038/nrc3278.
38. Hayes J D, McMahon M, Chowdhry S, et al. Cancer chemoprevention mechanisms mediated through the Keap1–Nrf2 pathway. *Antioxid Redox Signal* **2010**,13,1713–1748, DOI: 10.1089/ars.2010.3221.
39. Zhang P, Singh A, Yegnasubramanian S, et al. Loss of Kelch-like ECH-associated protein 1 function in prostate cancer cells causes chemoresistance and radioresistance and promotes tumor growth. *Mol. Cancer Ther* **2010**,9,336–346, DOI: 10.1158/1535-7163.MCT-09-0589.
40. Akhdar H, Loyer P, Rauch C, et al. Involvement of Nrf2 activation in resistance to 5-fluorouracil in human colon cancer HT-29 cells. *Eur J Cancer* **2009,**45(12),2219-27, DOI: 10.1016/j.ejca.2009.05.017.
41. Menegon S, Columbano A, Giordano S. The Dual Roles of NRF2 in Cancer. *Trends Mol Med* **2016,**22(7),578-93, DOI: 10.1016/j.molmed.2016.05.002.
42. Caamaño J, Hunter CA. NF-kappaB family of transcription factors: Central regulators of innate and adaptive immune functions. *Clin Microbiol Rev* **2002,**15,414-29.

43. Viennois E, Chen F, Merlin D. NF-κB pathway in colitis-associated cancers. *Transl Gastrointest Cancer* **2013,**2,21-9, DOI: 10.3978/j.issn.2224-4778. 2012.11.01.
44. Jurjus A ,Eid A, Al Kattar S, et al. Inflammatory bowel disease, colorectal cancer and type 2 diabetes mellitus: The links. *BBA Clin* **2015,**55,16-24, DOI: 10.1016/j.bbacli.2015.11.002.
45. Hayden MS, Ghosh. S. Shared principles in NF-kappaB signaling. *Cell.* **2008**,132(3),344-62, DOI: 10.1016/j.cell.2008.01.020
46. Ben-Neriah Y., Karin M. Inflammation meets cancer, with NF-[Kappa] B as the matchmaker. *Nature Immunology* **2011,**19,12(8):715-23, DOI: 10.1038/ni.2060.
47. Min C, Eddy S F, Sherr D H, et al. NF-κB and epithelial to mesenchymal transition of cancer. *Journal of Cellular Biochemistry* **2008**,104(3),733-44, DOI: 10.1002/jcb.21695.
48. Erez N., Truitt M., Olson P., et al. Cancer-Associated Fibroblasts are Activated in Incipient Neoplasia to Orchestrate Tumor-Promoting Inflammation in an NF-κB-Dependent Manner, *Cancer Cell* **2010**,17(2),135-47, DOI: 10.1016/j.ccr.2009.12.041.
49. Sena P, Mariani F, Mancini S, et al. Autophagy is upregulated during colorectal carcinogenesis, and in DNA microsatellite stable carcinomas. *Oncol Rep* **2015**,34(6),3222-30. DOI: 10.3892/or. 2015.4326.
50. Eray M M, Matto N, Kaartinen L, et al. Flow cytometric analysis of apoptotic subpopulations with a combination of Annexin V-FITC, propidium iodide, and SYTO 17. *Cytometry* **2001**,43, 134-142.